ApoA-I deficiency in mice is associated with redistribution of apoA-II and aggravated AApoAII amyloidosis[S]

Yaoyong Wang (王耀勇), Jinko Sawashita (澤下仁子), Jinze Qian (钱金泽), Beiru Zhang (张蓓茹), Xiaoying Fu (付笑影), Geng Tian (田耕), Lei Chen (陈磊), Masayuki Mori (森 政之), and Keiichi Higuchi (樋口京一)[1]

Department of Aging Biology, Institute on Aging and Adaptation, Graduate School of Medicine, Shinshu University, Matsumoto, Japan

Abstract Apolipoprotein A-II (apoA-II) is the second major apolipoprotein following apolipoprotein A-I (apoA-I) in HDL. ApoA-II has multiple physiological functions and can form senile amyloid fibrils (AApoAII) in mice. Most circulating apoA-II is present in lipoprotein A-I/A-II. To study the influence of apoA-I on apoA-II and AApoAII amyloidosis, apoA-I-deficient (C57BL/6J.*Apoa1*$^{-/-}$) mice were used. *Apoa1*$^{-/-}$ mice showed the expected significant reduction in total cholesterol (TC), HDL cholesterol (HDL-C), and triglyceride (TG) plasma levels. Unexpectedly, we found that apoA-I deficiency led to redistribution of apoA-II in HDL and an age-related increase in apoA-II levels, accompanied by larger HDL particle size and an age-related increase in TC, HDL-C, and TG. Aggravated AApoAII amyloidosis was induced in *Apoa1*$^{-/-}$ mice systemically, especially in the heart. These results indicate that apoA-I plays key roles in maintaining apoA-II distribution and HDL particle size. Furthermore, apoA-II redistribution may be the main reason for aggravated AApoAII amyloidosis in *Apoa1*$^{-/-}$ mice. These results may shed new light on the relationship between apoA-I and apoA-II as well as provide new information concerning amyloidosis mechanism and therapy.—Wang, Y., J. Sawashita, J. Qian, B. Zhang, X. Fu, G. Tian, L. Chen, M. Mori, and K. Higuchi. **ApoA-I deficiency in mice is associated with redistribution of apoA-II and aggravated AApoAII amyloidosis. *J. Lipid Res.* 2011.** 52: **1461–1470.**

Supplementary key words apolipoproteins • cholesterol • lipids • distribution • age • amyloid heart disease

HDL contains two major proteins, apoA-I and apoA-II, which compose about 70% and 20%, respectively, of the total HDL protein mass in humans. Both apoA-I and apoA-II have important physiological functions in lipid transport and metabolism. ApoA-I is distributed approximately equally between lipoprotein A-I (LpA-I) and lipoprotein A-I/lipoprotein A-II (LpA-I/A-II), whereas virtually all apoA-II is found with LpA-I/A-II (1). LpA-I is a major component of both HDL_2 and HDL_3, while LpA-I/A-II is found predominantly in HDL_3 (1). This distribution suggests that there is a close relationship between these two apolipoproteins.

ApoA-I, the major HDL protein in all vertebrates reported to date (2), plays crucial roles in lipid transport and metabolism by activating LCAT and promoting cholesterol efflux from peripheral tissues (3). Abundant data show that apoA-I has protective effects against atherosclerosis and cardiovascular disease in humans and mice, mainly by enhancing reverse cholesterol transport (RCT) and anti-inflammatory, antioxidant, or nitric-oxide-promoting properties (4). Clinically, the majority of patients with severe HDL and apoA-I deficiencies suffer from premature atherosclerosis (5). The negative correlation between plasma HDL cholesterol (HDL-C) concentrations and atherosclerosis is not observed in all disorders involving apoA-I deficiency, however (4). There are reports of mutations in the *Apoa1* gene that cause severe reductions in HDL-C concentrations in plasma but do not appear to increase coronary risk (6). In addition, apoA-I deficiency alone does not promote development of atherosclerotic lesions in B6/129 mice (7). Indeed, studies with trans-

This work was supported by the Ministry of Education, Culture, Sports, Science, and Technology of Japan, Grants-in-Aid for Scientific Research (B) 20300144 and Science Research on Priority Areas 22020015, and by grants from the Intractable Disease Division, the Ministry of Health, Labor, and Welfare to the Research Committees for Amyloidosis.

Manuscript received 28 November 2010 and in revised form 26 May 2011.

Published, JLR Papers in Press, May 26, 2011
DOI 10.1194/jlr.M013235

Abbreviations: AA, reactive amyloidosis; AApoAII, senile amyloid fibril; AI, amyloid index; AL, primary amyloidosis; apoA-I, apolipoprotein A-I; apoA-II, apolipoprotein A-II; CETP, cholesteryl ester transfer protein; DDW, distilled deionized water; FAP, polyneuropathy; HDL-C, HDL cholesterol; Lp, lipoprotein; LPS, lipopolysaccharides; RCT, reverse cholesterol transport; SAM, senescence-accelerated mouse; SPF, specific pathogen free; TC, total cholesterol; TG, triglyceride; WT, wild-type.

[1] To whom correspondence should be addressed.
e-mail: keiichih@shinshu-u.ac.jp

[S] The online version of this article (available at http://www.jlr.org) contains supplementary data in the form of one figure and one table.

genic mice highlight the physiological redundancy of HDL apolipoproteins (8). In addition to apoA-I, other apolipoproteins, such as apoE, apoA-II (9), and apoA-IV, are active in inducing cholesterol efflux from cells and may play important roles in substituting for the loss of apoA-I (10).

ApoA-II, the second most abundant protein present in human, mouse, rat, and fish plasma HDL (11), was long considered to be of minor physiologically importance in lipoprotein metabolism because apoA-II deficiency is not associated with a high susceptibility to coronary heart disease (12). However, recent studies show that apoA-II plays multiple metabolic roles in maintaining the plasma HDL pool (13–15), promoting obesity and insulin resistance (15, 16), augmenting monocyte responses to lipopolysaccharides (LPS) (17), and decreasing triglyceride catabolism, mainly by impairing lipoprotein lipase (LPL) activity (13). Although human apoA-II is either atheroprotective or pro-atherogenic in transgenic mice, depending on an atherogenic diet (18), mouse apoA-II is pro-atherogenic in chow-fed transgenic mice (19).

In human hereditary amyloidosis, a rare disorder that may cause progressive and life-threatening organ dysfunction, apoA-II can form AApoAII amyloid fibrils, which are mainly deposited in the kidney (20). In mice, apoA-II is a precursor of senile amyloid fibrils (AApoAII), which were first isolated from a senescence-accelerated inbred strain (SAMP1) having severe amyloidosis and were later found to be present universally in mice (21). Mouse AApoAII amyloidosis fibrils are spontaneously deposited systemically (excluding the brain) in an age-associated manner (21), resulting in a 20% shortened life span for R1.P1-*Apoa2*^{c} mice (22). In laboratory mice, there are three major alleles for *Apoa2*: *Apoa2*^{a}, *Apoa2*^{b}, and *Apoa2*^{c} (21, 23). We confirmed that strains carrying *Apoa2*^{a} and *Apoa2*^{c} are more susceptible to AApoAII amyloidosis than strains having *Apoa2*^{b} (14, 21, 23, 24).

To date, the influence of apoA-I on apoA-II is not clear. Although LpA-II, which lacks apoA-I and contains apoA-II as the main apolipoprotein constituent, was found in apoA-I-deficient patients (25), there are no detailed data concerning the distribution of apoA-II. For mice lacking apoA-I, apoE is confirmed to increase in compensation, although whether this also occurs for apoA-II is not known (7, 9). Recently, it was shown that apoA-I may also affect amyloidosis pathogenesis (26). ApoA-I can bind amyloid β (Aβ), and decrease Aβ-induced cytotoxicity in vitro, as well as attenuate formation of Aβ amyloid deposits on central nervous system blood vessel walls in vivo (26). However, there are few studies concerning the role of ApoA-I in other amyloidoses, including those associated with pathological disorders, such as primary (AL) amyloidosis, reactive (AA) amyloidosis, polyneuropathy (FAP), prion diseases, and familial, systemic, and sporadic amyloidosis.

Using C57BL/6J.*Apoa1*$^{-/-}$ mice (with *Apoa2*^{a} allele), we confirmed that apoA-I deficiency results in significantly reduced plasma levels of TC, HDL-C, and TG, as well as a 2-fold increased apoE level that was previously described by other studies (7). Unexpectedly, we also found *i*) age-related increases in the levels of plasma apoA-II, TC, HDL-C, and TG; *ii*) redistribution of apoA-II and larger HDL particles; and *iii*) aggravated systemic AApoAII amyloidosis and heart amyloidosis in *Apoa1*$^{-/-}$ mice. These results prompted us to explore how the loss of apoA-I affects the metabolism of apoA-II.

MATERIALS AND METHODS

Animals

C57BL/6J mice were purchased from Japan SLC, Inc. (Hamamatsu, Japan), and C57BL/6J.*Apoa1*$^{-/-}$ mice (B6.129P2-*Apoa1*^{tm1Unc}/J) were purchased from Jackson Laboratories (Bar Harbor, ME). The *Apoa1*^{tm1Unc} mutant strain was developed in the laboratory of Dr. Nobuyo Maeda (27). The C57BL/6J strain was produced by backcrossing the *Apoa1*^{tm1Unc} mutation 10 times to C57BL/6J inbred mice. Mice were maintained by sister-brother matings under specific pathogen free (SPF) conditions at 24 ± 2°C with a light-controlled regimen (12 h light/dark cycle). Mouse pups were weaned at four weeks and then fed a commercial diet containing 5.6% fat (C18:2 linoleic acid, 48.4%; C18:1 linoleic acid, 23.2%; C16 palmitic acid, 14.1%; C18:3 linolenic acid, 4%; C18 stearic acid, 2.5%; C20:5 eicosapentaenoic acid, 1.6%; C22:6 docosahexaenoic acid, 1.4%; C16:1 palmitoleic acid, 1.4%; C14 myristic acid, 0.4%; and others, 2.0%) that was purchased from Oriental Yeast (Tokyo, Japan). Tap water was provided ad libitum. Only female mice were used in this study to avoid AA amyloidosis or other adverse impacts caused by fighting and other behaviors among mice reared in the same cage. Mice were euthanized by cardiac puncture under diethyl ether anesthesia. All experimental procedures were carried out in accordance with the Regulations for Animal Experimentation of Shinshu University.

Lipoprotein quantity, HDL particle size, and distribution of plasma lipids

After an overnight fast, mice were sacrificed for plasma collection and other experiments, such as pathologic investigation. Levels of plasma TC, HDL-C, and TG were detected in duplicate determinations using commercially available kits (total cholesterol E-test kit, 439-17501; HDL-cholesterol E-test kit, 431-52501; Triglyceride E-test kit, 432-40201; Wako Pure Chemical Industries, Osaka, Japan). Pooled plasma of some groups was also analyzed with a dual-detection, high-performance liquid chromatography (HPLC) system (Liposearch System, Skylight Biotech, Inc., Akita, Japan) (28). HDL-C values determined by the HDL-cholesterol E-test kit were confirmed by HPLC procedures (supplemental Table I).

To determine HDL particle size, plasma (5 μl for WT mice; 10 μl for *Apoa1*$^{-/-}$ mice) prestained for lipids with Sudan Black B was electrophoresed on a nondenaturing PAGE gel with a 5-15% linear polyacrylamide gradient. Electrophoresis was carried out at 25 mA for 2 h (14, 29). The distribution of apoA-I, apoA-II, apoE, apoA-IV, and apoC- II protein among the HDL species was determined by Western blot analysis of 0.5, 2, 1, 1, and 2 μl plasma, respectively, separated by nondenaturing PAGE. To further determine the cholesterol profiles in plasma lipoproteins, pooled plasma from mice (n = 3) was analyzed with HPLC. Isolated HPLC fractions with different particle diameters (ranging from 7.6 nm to >80 nm) from 4 μl pooled plasma were separated by SDS-PAGE, and apoA-II protein was determined by Western blot analysis.

Analysis of apoE and apoA-II plasma concentrations

Plasma (1 and 2 μl for apoE and apo-II, respectively) from C57BL/6J and *Apoa1*$^{-/-}$ mice was separated by electrophoresis at 15 mA for 6 h on Tris-Tricine/SDS-16.5% polyacrylamide gels

(SDS-PAGE). After electrophoresis, proteins were transferred to a polyvinylidene difluoride (PVDF) membrane using a semidry Western blot apparatus at 150 mA for 1.5 h. The membrane was then probed with goat anti-apolipoprotein E polyclonal antibody diluted 1:2,000 (AB947, Chemicon International) or polyclonal rabbit anti-mouse apoA-II diluted 1:1,500 in 3% skim milk in PBS containing 0.1% Tween-20 (T-PBS) for 1 h at room temperature. Subsequently, membranes were incubated for 1 h with horseradish peroxidase (HRP)-conjugated anti-goat IgG solution (1:3,000) or anti-rabbit IgG solution (1:3,000). ApoE and ApoA-II were detected with the enhanced chemiluminescence (ECL) system and quantified using a densitometric image analyzer with NIH Image version 1.61 (Bethesda, MD). Pooled plasma from two-month-old wild-type (WT) mice was used as standard plasma to calculate the relative apoE concentration. Plasma with 25 mg/dl apoA-II concentration, determined by purified apoA-II protein (30), was used as standard plasma to calculate the concentration of apoA-II (supplemental Fig. I).

Anti-apoA-II antiserum was produced in rabbits by injecting type C apoA-II protein purified from AApoAII amyloid fibrils deposited in the liver of a SAMP1 mouse (31). This anti-apoA-II antiserum can react specifically with plasma type A, type B, and type C apoA-II on a Western blot. This anti-apoA-II antiserum can also react specifically with type A, type B, and type C AApoAII fibrils on a Western blot or immunohistochemistry (14, 24, 32).

Analysis of *Apoa2* mRNA expression in the liver and heart

Total RNA was extracted from livers or hearts (including the atrium cordis and ventriculus cordis) of two- and six-month-old mice using TRIzol Reagent (Invitrogen), followed by treatment with DNA-Free (Applied Biosystems, Foster City, CA) to remove contaminating DNA. Then it was subjected to reverse transcription using an Omniscript RT kit (Applied Biosystems) with random primers (Applied Biosystems). The cycling parameters for reverse transcriptase-polymerase chain reaction (RT-PCR) amplification were initial denaturation for 1 min at 94°C, followed by 23 cycles of 30 s at 94°C, 30 s at 60°C, and 45 s at 72°C for GAPDH; 24 cycles for hepatic *Apoa1*; 21 cycles for hepatic *Apoa2*; and 32 cycles for cardiac *Apoa2*. Quantitative real-time RT-PCR analysis was carried out using an ABI PRISM 7500 Sequence Detection System (Applied Biosystems) with SYBR Green (Takara Bio, Tokyo, Japan), and values were normalized with respect to GAPDH. The following primers were used: *Apoa1*-F 5′-GTGGCTCTGGTCTTC-CTGAC-3′, *Apoa1*-R 5′-ACGGTTGAACCCAGAGTGTC-3′ (218 bp); *Apoa2*-F 5′-GCCTGTTCACTCAGTACTTTCAG-3′ and *Apoa2*-R 5′-CAGACTAGTTCCTGCTGACC-3′ (155 bp); and GAPDH-F 5′-TGCACCACCAACTGCTTAG-3′ and GAPDH-R 5′-GGATGCAGGGATGATGTTC-3′ (177 bp).

Isolation of amyloid fibrils

AApoAII(C) fibrils were isolated from the liver of a 12-month-old R1.P1-*Apoa2*^{f} mouse, a congenic strain carrying the amyloidogenic *Apoa2*^{f} allele from the SAMP1 strain in the genetic background of SAMR1 (33), which also had severe amyloid deposition induced by intravenous injection of AApoAII(C) fibrils. AApoAII(A) fibrils were isolated from the liver of a 12-month-old C57BL/6 mouse, which had severe amyloid deposition induced by intravenous injection of AApoAII(C) amyloid fibrils. Both amyloid fibril fractions were isolated by Pras's method with some modification (14). Isolated amyloid fibrils were suspended in distilled deionized water (DDW) at a concentration of 1.0 mg/ml and kept at −70°C. Of this mixture, 1 ml was placed in a 1.5 ml Eppendorf tube and sonicated on ice for 30 s with an ultrasonic homogenizer VP-5S (Tietech Co., Ltd., Tokyo, Japan) at maximum power. This procedure was repeated five times at 30 s intervals. Sonicated AApoAII samples were used immediately.

Induction of amyloidosis in C57BL/6J.*Apoa1*$^{-/-}$ mice

Previously we have shown that AApoAII(A) amyloidosis could be induced by AApoAII(C) amyloid fibrils by cross-seeding, and confirmed that the depositions in C57BL/6 mice with *Apoa2*^{a} were endogenous AApoAII(A) amyloid fibrils (32). Therefore, to induce AApoAII amyloidosis, 10 or 100 μg sonicated AApoAII(C) amyloid fibrils suspended in 100 μl DDW were injected into the tail vein of two-month-old female Apoa1$^{-/-}$ and WT mice. After two or four months, the treated mice were euthanized, and amyloid deposition was determined. We also induced amyloidosis by self-seeding with AApoAII(A) amyloid fibrils and compared the amyloid deposition. Control mice were injected with 100 μl DDW containing no amyloid fibrils. The mice were euthanized by cardiac puncture under diethyl ether anesthesia, and major tissues were fixed in 10% neutral buffered formalin, embedded in paraffin, and cut into 4 μm sections for Congo Red staining and immunohistochemistry.

Detection of amyloid deposition

Deposition of amyloid fibrils in each mouse was identified by polarizing microscopy using Congo Red-stained sections, where green birefringence indicates the presence of amyloid. The intensity of amyloid deposition was determined semiquantitatively using the amyloid index (AI) as a parameter. The AI parameter represents the average degree of deposition, graded from 0 to 4, in the seven organs (heart, liver, spleen, stomach, intestine, tongue, and skin) examined in Congo Red-stained sections. Amyloid fibril proteins were identified by immunohistochemistry using the avidin-biotin horseradish peroxidase complex method. Specific antisera against mouse AApoAII and mouse AA were used (31). Tissues were examined by two independent observers who were blinded to the experimental protocol.

Statistical analysis

We used the StatView software package (Abacus Concepts, Berkley, CA) for data analysis. All data are presented as the mean ± SD. Because the AI is nonlinear, the AIs of different groups of mice were compared using the nonparametric Mann-Whitney *U*-test. One-way Anova and Student's *t*-test were used for all data except AI.

RESULTS

ApoA-I deficiency results in age-related increases in plasma apoA-II, cholesterol, and lipids

To determine whether apoA-I deficiency influences the metabolism of apoA-II and apoE, the major protein constituents of HDL from *Apoa1*$^{-/-}$ mice (7, 9), we determined the plasma levels of apoA-I, apoA-II, and apoE in two-, four-, and six-month-old WT and *Apoa1*$^{-/-}$ mice by Western blot analysis after separating plasma proteins by SDS-PAGE. In WT mice, plasma levels of apoA-I (data not shown), apoA-II, and apoE remained effectively constant across the ages tested. In contrast, for *Apoa1*$^{-/-}$ mice, apoA-I protein was absent, and apoE levels were about 2-fold higher compared with WT mice. Furthermore, the level of apoE in *Apoa1*$^{-/-}$ mice did not change significantly with age (**Fig. 1A**, C). Although the level of apoA-II decreased in two-month-old *Apoa1*$^{-/-}$ mice (from 23.9 ± 3.3 to 18.9 ± 2.8 mg/dl), there was a significant increase as *Apoa1*$^{-/-}$ mice aged (21.0 ± 6.0 and 31.1 ± 5.8 mg/dl at four and six months, respectively) (Fig. 1A, B).

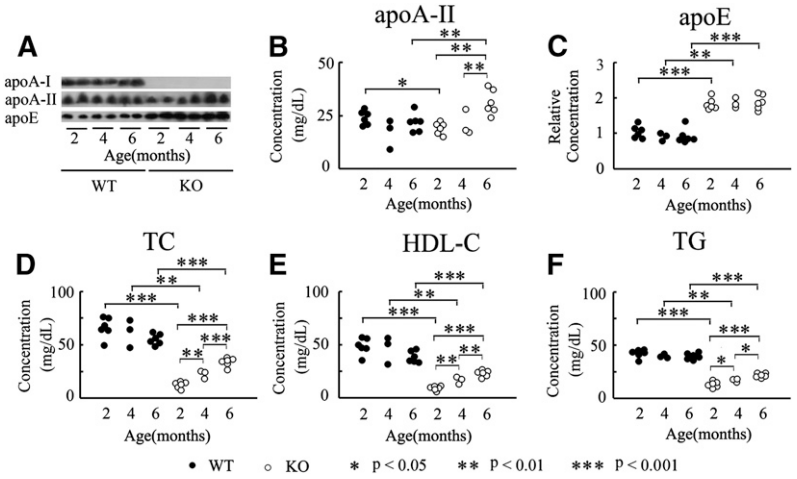

Fig. 1. Plasma apolipoproteins, TC, HDL-C and TG in Apoa1$^{-/-}$ mice at two, four, and six months. A: ApoA-I, apoA-II. and apoE from WT and *Apoa1*$^{-/-}$ mice were detected with specific antisera after SDS-PAGE and Western blot. B, C: Plasma concentrations of apoA-II and apoE were quantitated using a densitometric image analyzer with NIH Image. D, E, F: Plasma concentrations of TC, HDL-C, and TG. KO, *Apoa1*$^{-/-}$; n = 3-6.

We confirmed that *Apoa1*$^{-/-}$ mice had highly significant reductions in plasma TC, HDL-C, and TG (Fig. 1D–F), as previously described in other studies (7). For example, in two-month-old *Apoa1*$^{-/-}$ mice, TC and HDL-C levels decreased to about one fifth of normal levels (from 66.4 ± 9.7 to 12.7 ± 3.1 mg/dl for TC, and from 49.0 ± 7.8 to 9.4 ± 2.3 mg/dl for HDL-C), while TG was one third that of normal levels (from 42.5 ± 4.0 to 13.4 ± 2.8 mg/dl). For WT mice, plasma levels of TC, HDL-C, and TG did not change significantly as the mice aged. In contrast, *Apoa1*$^{-/-}$ mice displayed significant increases in levels of plasma TC, HDL-C, and TG with age. Levels of plasma TC increased to 22.8 ± 3.8 mg/dl at four months, and to 34.1 ± 4.0 mg/dl at six months. HDL-C plasma levels increased to 17.1 ± 3.4 mg/dl at four months, and to 23.4 ± 3.0 mg/dl at six months. Levels of plasma TG were also raised significantly, from 17.4 ± 1.6 mg/dl at four months to 22.0 ± 2.0 mg/dl at six months (Fig. 1D–F).

ApoA-I deficiency results in larger HDL particle size and redistribution of apoA-II among HDL

To elucidate the effect of apoA-I deficiency on lipoprotein particles and the distribution of other important apolipoproteins, we determined HDL particle size by nondenaturing PAGE of plasma prestained with Sudan Black B. We performed Western blot analysis of plasma apolipoproteins following separation by nondenaturing PAGE. In this experiment, HDL appeared monotonic (**Fig. 2A**), and we marked size classes of HDL_1, HDL_2, and HDL_3 based on the distributions of apoA-I and apoA-II in WT mice and our previously reported results (14, 29).

There were clear differences between HDL species for WT and *Apoa1*$^{-/-}$ mice, with HDL_3 and HDL_2 being the predominant form observed in WT mice. Although there was no clear band corresponding to HDL on nondenaturing PAGE for two-month-old *Apoa1*$^{-/-}$ mice due to low plasma lipid levels, for four- and six-month-old *Apoa1*$^{-/-}$

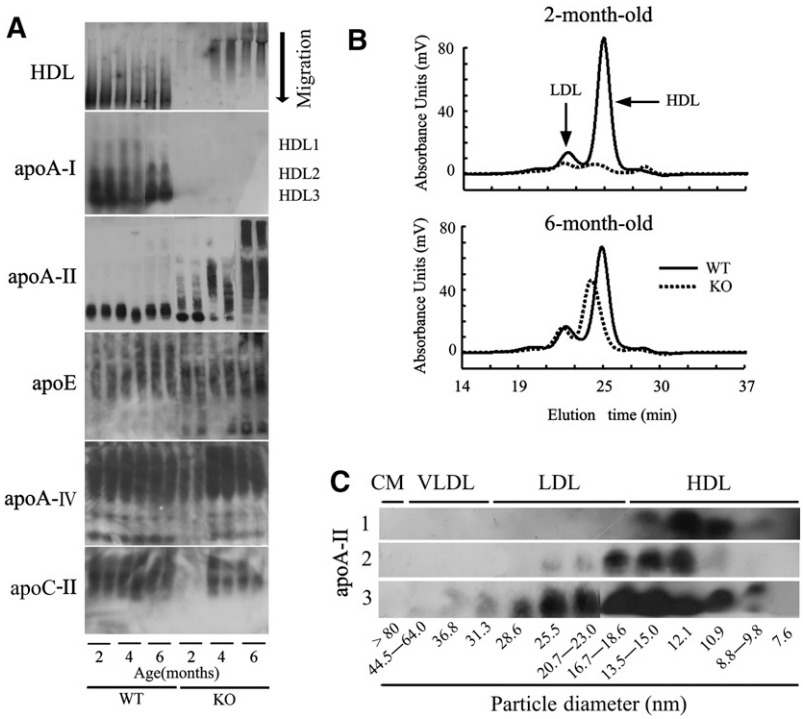

Fig. 2. ApoA-I deficiency results in redistribution of apoA-II and larger HDL particles. A: HDL particle size and apolipoprotein distribution among HDL species were analyzed by nondenaturing 5-15% PAGE. To detect HDL particle size, 5 or 10 μl plasma from two-, four-, or six-month-old WT or *Apoa1*$^{-/-}$ mice were prestained with Sudan Black B. ApoA-I, apoA-II, apoE, apoA-IV, and apoC-II protein distribution among HDL species was detected with specific antisera following Western blot. B: Cholesterol profiles in plasma lipoproteins were analyzed using a dual detection HPLC system. C: Isolated HPLC fractions of 4 μl pooled plasma were separated by SDS-PAGE, and apoA-II protein was determined by Western blot analysis. Line 1: Two-month-old WT mice. Line 2: Two-month-old *Apoa1*$^{-/-}$ mice. Line 3: Six-month-old *Apoa1*$^{-/-}$ mice.

mice, the predominant form was HDL_1, rather than HDL_3 and HDL_2 (Fig. 2A). ApoA-I was distributed mainly in HDL_3 and HDL_2 in WT mice, while there was no apoA-I in *Apoa1*$^{-/-}$ mice, as expected. Although apoA-II was largely found with HDL_3 in WT and two-month-old *Apoa1*$^{-/-}$ mice, it was unexpectedly found mainly with HDL_1 in four- and six-month-old *Apoa1*$^{-/-}$ mice. Although there was no clear band for apoA-IV and apoC-II from two-month-old *Apoa1*$^{-/-}$ mice due to low plasma concentration as described (7, 9), it was shown that apoA-IV was distributed extensively with HDL, while apoE and apoC-II were distributed mainly with HDL_1 in both WT mice and *Apoa1*$^{-/-}$ mice. As such, apoA-I deficiency resulted in redistribution of apoA-II in an age-dependent manner, but it had no obvious influence on the distribution of other apolipoproteins detected in this study (Fig. 2A).

To confirm this result, pooled plasma from two- and six-month-old WT and *Apoa1*$^{-/-}$ mice was analyzed with a dual-detection HPLC system. For WT mice, there was no marked age-dependent change in the quantity of cholesterol and HDL particle size. In contrast, *Apoa1*$^{-/-}$ mice showed a marked increase in the quantity of cholesterol and HDL particle size between two and six months of age (Fig. 2B). Separation of isolated HPLC fractions by SDS-PAGE and subsequent Western blot analysis of apoA-II protein clearly showed that apoA-II existed mainly in HDL particles with diameters ranging from 10.9 to 12.1 nm in two-month-old WT mice, while two-month-old *Apoa1*$^{-/-}$ mice had larger HDL and LDL particles with diameters from 12.1 to 18.6 nm. Particle sizes were further increased for six-month-old *Apoa1*$^{-/-}$ mice, which had HDL and LDL particles from 10.9 to 28.6 nm in diameter (Fig. 2C).

ApoA-I deficiency results in aggravated AApoAII amyloidosis

In this experiment, we used AApoAII(C) amyloid fibrils to induce AApoAII amyloidosis, and we used AApoAII(A) amyloid fibrils to confirm the results. Amyloid deposition in tissues was determined by Congo Red staining and immunohistochemistry two and/or four months after injection. As a control, mice were injected with 100 μl distilled water, which produced no amyloid deposition in WT or *Apoa1*$^{-/-}$ mice two and four months after injection (data not shown). Systemic amyloid depositions were induced by administration of 10 or 100 μg AApoAII(C) amyloid fibrils in WT and *Apoa1*$^{-/-}$ mice. Immunohistochemical staining for amyloid deposition was positive with anti-AApoAII antiserum but negative with anti-AA antiserum (data not shown).

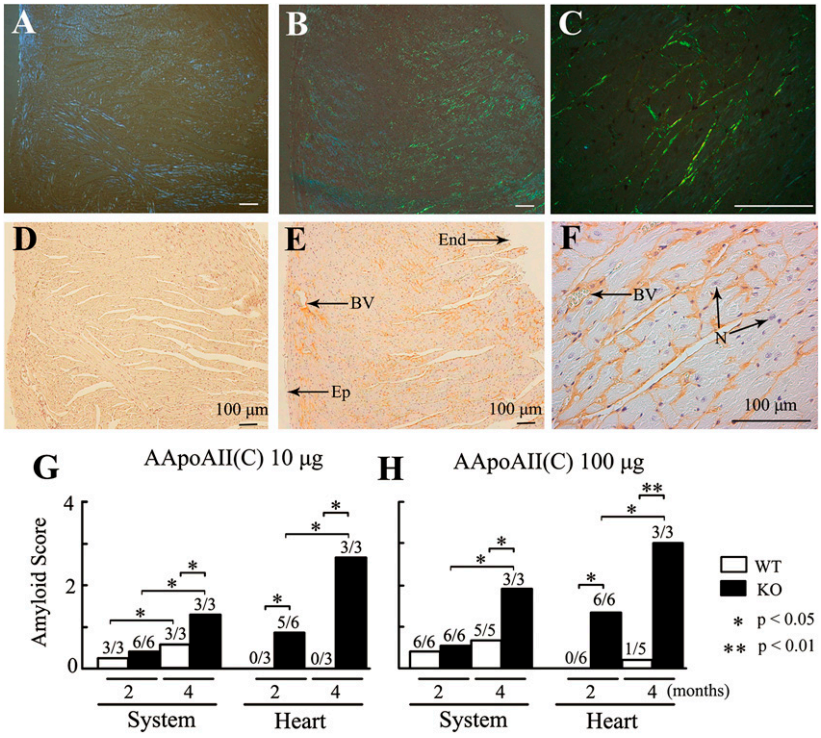

Fig. 3. Aggravated AApoAII amyloid deposition was induced in *Apoa1*$^{-/-}$ mice. Four months after injection of 100 μg AApoAII(C) amyloid fibrils, heavy amyloid deposition was observed in hearts of six-month-old *Apoa1*$^{-/-}$ mice (B, C, E, F) but not of WT mice (A, D). Amyloid deposits in the blood vessels and interstitial tissues surrounding myocardial fibers of *Apoa1*$^{-/-}$ mice (B, C) displayed green birefringence in Congo Red-stained sections. Amyloid deposition was identified using anti-apoA-II antiserum (E, F). G, H: The grade of amyloid deposition in the heart and system was determined using Congo Red-stained sections two and four months after mice were injected with 10 or 100 μg AApoAII(C) amyloid fibrils. Systemic amyloid score represents the average degree of deposition, graded 0 to 4, in the seven organs examined (heart, liver, spleen, stomach, intestine, tongue, and skin). Numbers above the columns represent amyloid positive mice/examined mice. BV, blood vessel; End, endocardium; Ep, epicardium; N, nucleus.

In WT mice, injection of 10 μg AApoAII(C) amyloid fibrils induced amyloid deposition that was observed only in the tongue (3/3) (AI = 0.24) two months after injection; by four months postinjection, deposits were seen in the stomach (3/3) and intestine (3/3) as well as more deposits in the tongue (3/3) (AI = 0.57). In contrast, aggravated amyloid deposits were observed in the tongue (6/6), heart (5/6), and stomach (3/6) of *Apoa1*$^{-/-}$ mice two months after injection (AI = 0.36), and additional deposits were found in the tongue (3/3), heart (3/3), stomach (3/3), intestine (3/3), liver (3/3), and skin (1/3) (AI = 1.29) four months after injection.

Like R1.P1-*Apoa2*^{c} mice (34), the degree of amyloid deposition increased in a dose-dependent manner in both WT and *Apoa1*$^{-/-}$ mice. In WT mice, administration of 100 μg AApoAII(C) amyloid fibrils induced amyloid deposition in the tongue (6/6) and stomach (5/6) (AI = 0.41) two months after injection and further in the tongue (5/5), stomach (4/5), intestine (3/5), liver (3/5), and a few in the heart (1/5) (AI = 0.71) four months postinjection. On the other hand, injection of 100 μg AApoAII amyloid fibrils in *Apoa1*$^{-/-}$ mice aggravated the amyloid deposits observed in the tongue (6/6) and produced deposits in the heart (5/6) and stomach (3/6) (AI = 0.36) after two months; after four months, deposits were detected in the tongue (3/3), heart (3/3), stomach (3/3), intestine (3/3), liver (3/3), spleen (2/3), and skin (1/3) (AI = 1.90) (**Fig. 3**, **Table 1**).

To confirm our result in *Apoa1*$^{-/-}$ mice, 10 or 100 μg endogenous AApoAII(A) amyloid fibrils were injected. Two months after injection, mice were euthanized, and the degree of amyloid deposition was determined. Again, we found that more aggravated amyloidosis was induced in *Apoa1*$^{-/-}$ mice compared with WT mice following injection of AApoAII(A) amyloid fibrils (Table 1). We did not perform the experiment of four-month treatment of AApoAII(A).

In summary, we confirmed that regardless of amyloid fibril type (AApoAII(C) versus AApoAII(A) or quantity (10 versus 100 μg), and the amount of time following treatment (two versus four months), more AApoAII amyloid deposition was induced by fibril injection in *Apoa1*$^{-/-}$ mice compared with WT mice.

TABLE 1. Induction of amyloidosis by the injection of two kinds of AApoAII amyloid fibrils

Injected		Amyloid Score[a] (2M)								Amyloid Score (4M)							
Strain	Amyloid fibrils	N	Heart	Liver	Spleen	Stomach	Intestine	Tongue	Skin	AI[b]	N	Heart	Liver	Spleen	Stomach	Intestine	Tongue	Skin	AI
WT	AApoAII(C) 10 μg	3	0.0	0.0	0.0	0.0	0.0	1.7	0.0	0.2^{c}	3	0.0	0.0	0.0	1.0	1.0	2.0	0.0	0.6^{d}
WT	AApoAII(A) 10 μg	3	0.0	0.0	0.0	0.3	0.0	2.0	0.0	0.3^{e}									
WT	AApoAII(C) 100 μg	6	0.0	0.0	0.0	0.8	0.0	2.0	0.0	0.4^{f}	5	0.2	0.8	0.0	1.0	0.6	2.4	0.0	0.7^{g}
WT	AApoAII(A) 100 μg	3	0.0	0.0	0.0	0.7	0.0	2.0	0.0	0.4^{h}									
KO	AApoAII(C) 10 μg	6	0.8	0.0	0.0	0.5	0.0	1.2	0.0	0.4^{i}	3	2.7	1.3	0.0	1.7	1.0	2.0	0.3	1.3^{j}
KO	AApoAII(A) 10 μg	3	2.0	0.0	0.0	0.0	0.0	1.7	0.0	0.5^{k}									
KO	AApoAII(C) 100 μg	6	1.3	0.0	0.0	0.8	0.0	1.7	0.0	0.5^{l}	3	3.0	2.0	0.7	3.0	2.0	2.3	0.3	1.9^{m}
KO	AApoAII(A) 100 μg	3	2.0	0.0	0.0	1.0	0.0	2.3	0.0	0.8^{n}									

The AI of different groups of mice was compared using the nonparametric Mann-Whitney-test. Values with different letters (c versus d, f; d versus j; e versus k; f versus g; g versus m; h versus n; i versus j, k, l; j versus m; and l versus m) are significantly different ($P < 0.05$).

[a] Amyloid Score of each organ, graded 0 to 4, was determined after 2 and 4 months for each mouse injected with amyloid fibrils. Hea, heart; Liv, liver; Spl, spleen; Stm, stomach; Int, intestine; Ton, tongue; and Skn, skin.

[b] The AI (Amyloid Index) refers the average degree of deposition, graded 0 to 4, in the seven organs examined (heart, liver, spleen, stomach, intestine, tongue, and skin).

ApoA-I deficiency results in higher expression of hepatic and cardiac *Apoa2* mRNA

Although *Apoa2* mRNA is expressed in many organs, apoA-II is mostly synthesized by the liver (35). To elucidate the mechanism of elevated plasma apoA-II concentration and high sensitivity to AApoA-II amyloidosis in *Apoa1*$^{-/-}$ mice hearts, we determined the levels of hepatic and cardiac *Apoa2* mRNA in two- and six-month-old mice by RT-PCR and real-time PCR. In WT mice, levels of hepatic and cardiac *Apoa2* mRNA did not change until six months, when the level of cardiac *Apoa2* mRNA was about 5,000 times lower than hepatic *Apoa2* mRNA (data not shown). Interestingly, *Apoa1*$^{-/-}$ mice had higher expression of hepatic *Apoa2* mRNA (1.2 times at two months and 1.5 times at six months) and cardiac *Apoa2* mRNA (about 5 times at two and six months).

Aggravated AApoAII amyloidosis results in decreased HDL-C and apoA-II concentrations in *Apoa1*$^{-/-}$ mice

To evaluate how AApoAII amyloidosis induction affects the concentrations of HDL-C and the precursor protein apoA-II, serial plasma samples were evaluated two and four months after injection of 10 or 100 μg AApoAII(C) amyloid fibrils (1.5 times at six months) and cardiac *Apoa2* mRNA (about 5 times at two and six months) (**Fig. 4**).

In WT mice, there was no significant change in HDL-C and apoA-II concentrations two or four months after injection of 10 or 100 μg AApoAII(C) amyloid fibrils. In *Apoa1*$^{-/-}$ mice, there was no significant change in HDL and apoA-II plasma concentrations two months after fibril injection. After four months, however, there was a significant decrease in the plasma concentrations of HDL and apoA-II when 100 μg AApoAII(C) amyloid fibrils were injected, compared with control mice (**Fig. 5A**, B, D).

To determine whether AApoAII amyloidosis influences lipoprotein particles, we determined HDL particle size by nondenaturing PAGE. We observed no clear change in HDL sizes for either *Apoa1*$^{-/-}$ or WT mice (Fig. 5C), which was supported by HPLC analysis (data not shown).

DISCUSSION

In this study, we focused on how apoA-I deficiency influences apoA-II and AApoAII amyloidosis in mice. We confirmed that apoA-I deficiency resulted in a significant reduction of TC, HDL-C, and TG but increased plasma apoE levels (7, 9).Unexpectedly, we found that apoA-I deficiency results in *i*) age-related increases in apoA-II, TC, HDL-C; and TG plasma levels; *ii*) redistribution of apoA-II and larger-sized HDL particles; and *iii*) aggravated AApoAII amyloidosis and heart amyloidosis.

ApoA-I plays key roles in lipid transport and metabolism mainly by activating LCAT and maintaining RCT (3, 4). As such, it is not surprising that human apoA-I overexpression results in elevated HDL-C levels in mice (14) and that apoA-I-deficiency causes a marked reduction in HDL-C levels in humans and mice (5–7).

ApoA-II is also known to be important for RCT and maintaining the plasma HDL pool. Human apoA-II exerts at least part of its pro-atherogenic effect by counteracting the antioxidant properties of HDL, not by impairing macrophage-specific RCT (36, 37). Furthermore, in *hApoa2* transgenic mice, RCT from macrophages to liver and feces was enhanced under a chow-fed diet (38). On the other hand, mice that over express *mApoa2* have increased HDL-C (14), and apoA-II-deficient mice have dramatically decreased HDL-C (15).

In this study, we found that apoA-II levels in apoA-I-deficient mice at two and four months of age did not differ significantly from WT mice, but by six months of age, apoA-II levels markedly increased to about 1.5-fold more than in six-month-old WT mice. Although *Apoa2* mRNA is expressed in many organs, apoA-II is mostly synthesized by the liver (35). We found that there was a higher expression of hepatic *Apoa2* mRNA in apoA-I-deficient mice (1.2 and 1.5 times at two and six months, respectively). These changes may account for the age-dependent increase in apoA-II levels in apoA-I-deficient mice. In addition, there are other possibilities that could account for these changes, such as alterations in the secretion and metabolism of apoA-II in apoA-I-deficient mice. We believe that the increased apoA-II levels may play more important roles than simply substituting for the loss of apoA-I. The role of apoA-II during RCT and its powerful ability to impair LPL activity (13) may explain the observed age-related increases in plasma cholesterol and TG.

In humans and mice, most apoA-II exists as an integral protein constituent of LPA-I/A-II, which is present in HDL_3. Interestingly, LP A-II, a minor HDL species characterized by having apoA-II as its major protein constituent, was isolated from normolipidemic subjects and apoA-I-deficient patients (25). LP-A-II also can interact with other apolipoproteins to form LPA-II:B or LPA-II:B:C:D:E complexes in VLDL of apoA-I-deficient patients (25, 39). The lipid profile of LPA-II from apoA-I-deficient patients is characterized by a significantly higher percentage of triglycerides and a lower percentage of phospholipids compared with LPA-II from normolipidemic subjects (25). These differences suggest that human lipoprotein particles containing apoA-II from apoA-I-deficient patients have larger sizes than normal LPA-I/A-II particles. In this

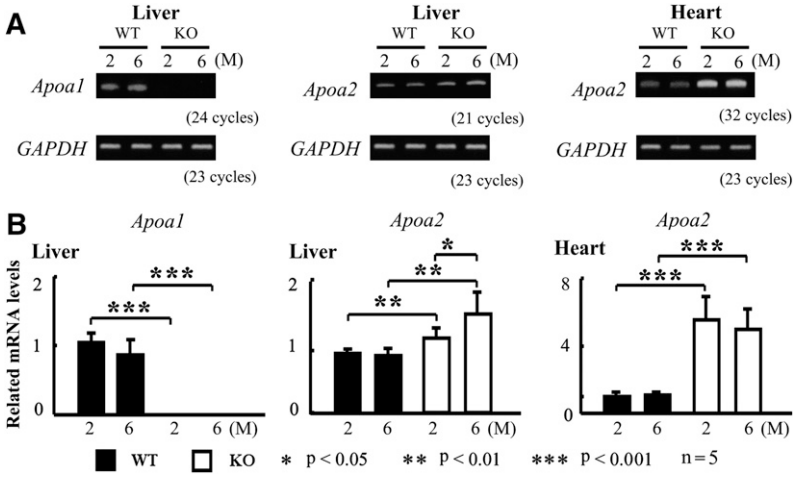

Fig. 4. ApoA-I deficiency results in higher expression of hepatic and cardiac *Apoa2* mRNA. Total RNA was extracted from livers and hearts of two- and six-month-old mice. After cDNA synthesis, expression of *Apoa1* and *Apoa2* mRNA was determined by RT-PCR analysis (A). Levels of *Apoa1* and *Apoa2* mRNA were detected by real-time PCR analysis (B).

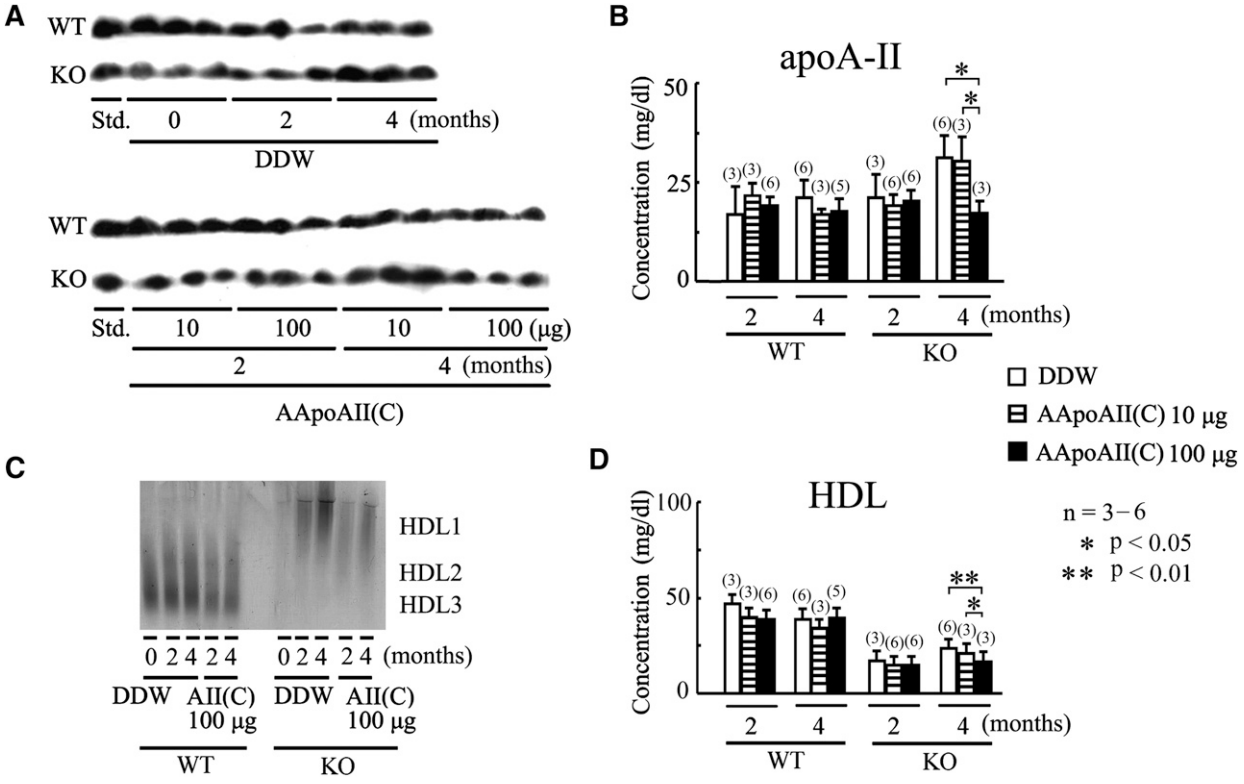

Fig. 5. Induction with AApoAII amyloid fibrils decreased apoA-II and HDL-C concentration in *Apoa1*$^{-/-}$ mice. Two and four months after mice were injected with DDW, 10 μg AApoAII(C) amyloid fibrils, or 100 μg AApoAII(C) amyloid fibrils, apoA-II and HDL-C concentrations were determined. A: ApoA-II was detected with specific antisera following SDS-PAGE and Western blot. B: The plasma concentrations of apoA-II were quantitated using a densitometric image analyzer with NIH Image. C: HDL particle size was analyzed by nondenaturing 5-15% PAGE using 5 or 10 μl plasma from WT or *Apoa1*$^{-/-}$ mice, respectively. D: HDL-C was determined by an enzymatic procedure. Values are means ± SD.

study, we clearly showed that apoA-II in *Apoa1*$^{-/-}$ mice mainly exists in HDL_3 at two months as expected, whereas the predominant species at four and six months is HDL_1. At the same time, the size of HDL from *Apoa1*$^{-/-}$ mice was larger compared with WT mice. Thus, it is possible that mouse apoA-II may form LP-A-II or interact with other apolipoproteins to form LP complexes in HDL. At present, there has been little research about the characteristics and functions of the apoA-II only lipoprotein. Further investigations of apoA-II could be helpful to understand the mechanism of larger HDL in apoA-I mutation in humans (40) and the relationship between apoA-I and other lipoproteins. ApoE is an important component of LP-A-II:B:C:D:E particles in apoA-I-deficient humans (25). In *Apoa1*$^{-/-}$ mice, apoE mainly exists in large HDL, and the 2-fold higher level of apoE suggests that apoE may play an important role in increasing HDL size and substituting for the loss of apoA-I. Because mice lack endogenous cholesteryl ester transfer protein (CETP), a hydrophobic plasma glycoprotein that promotes transfer of CE from HDL to apoB-containing lipoproteins (41), apoA-I-deficient mice have considerably higher HDL-C levels (>10 mg/dl) than apoA-I-deficient humans (<4 mg/dl). The lack of CETP in mice may also account for why apoA-I-deficient humans have decreased apoA-II in HDL, while we observed increased apoA-II in HDL from apoA-I-deficient mice. As complete apoA-I deficiency in humans is rare, it would be necessary to study the effects of reducing apoA-I levels on apoA-II- as well as heterozygous apoA-I-deficient mice, which may be an ideal model for further research.

Mouse AApoA-II amyloid is spontaneously deposited systemically in the body, although not in brain, in an age-associated manner (21). Exogenous amyloid fibrils could act as seeds (nuclei) that accelerate the conformational change of endogenous amyloid protein into fibril form. Regardless of the seed type [AApoAII(C) or AApoAII(A) amyloid fibrils], seed quantity (10 or 100 μg), or time after treatment (two or four months), more AApoAII amyloid deposition was induced in *Apoa1*$^{-/-}$ mice than in WT mice. This result may be due primarily to apoA-II redistribution rather than increased apoA-II concentrations, because aggravated AApoAII amyloidosis was induced in *Apoa1*$^{-/-}$ mice two months after treatment (i.e., at four months of age), a time when apoA-II levels in *Apoa1*$^{-/-}$ mice were no higher than that of four-month-old WT mice. This result indicates that apoA-II in LPA-I/A-II is more resistant to conformational changes from the normal host cellular protein to an abnormal form. In agreement with our results, low concentrations of HDL and apoA-I were shown to be highly correlated with the severity of Alzheimer's disease, likely because apoA-I can suppress Aβ in vitro and in vivo (26). These findings suggest that apoA-I may be a potential therapeutic target for human amyloidoses, such as Alzheimer's disease, AL and AA amyloidosis, and FAP.

In mice, AApoAII amyloid deposits first form in the tongue, stomach, and intestine, and then extend to other tissues, with the heart moderately susceptible to AApoAII amyloidosis (14). In this study, we showed that hearts of *Apoa1*$^{-/-}$ mice were highly susceptible to AApoAII amyloidosis. Why this result occurred is unclear, but one possible explanation is that apoA-I deficiency may alter the microenvironment of the heart. The heart has significant muscle content, but we noticed that there was no obvious AApoAII amyloid deposition in the muscle tissues from the tongues, intestines, and stomachs of *Apoa1*$^{-/-}$ mice (data not shown). As such, heart may have tissue specificity to AApoAII amyloidosis in *Apoa1*$^{-/-}$ mice. Although there is very low expression of *Apoa2* mRNA in the heart, we found that there was about 5-fold higher expression of cardiac *Apoa2* mRNA in *Apoa1*$^{-/-}$ mice. This higher endogenous apoA-II may, at least in part, account for the heart's higher susceptibility to AApoAII amyloidosis.

In humans, the heart is also highly vulnerable to some types of amyloidoses, such as AL and AA amyloidosis, FAP, and isolated atrial amyloidosis (42). There is no effective treatment for amyloid heart disease, which leads to an infiltrative/restrictive cardiomyopathy (42). Further research on apoA-I may help define the mechanism of amyloid heart disease and aid in the development of therapeutic strategies.

We also detected a significant decrease in HDL and apoA-II plasma concentrations four months after severe amyloidosis was induced in *Apoa1*$^{-/-}$ mice by injection of 100 μg AApoAII(C) amyloid fibrils. In earlier studies, we confirmed that the serum level of apoA-II decreased during amyloidosis in SAMP1 mice (43). Since aggravated AApoAII amyloidosis did not alter the synthesis of apoA-II but instead accelerated apoA-II catabolism (43), the decrease in HDL and apoA-II plasma concentrations may be the result of, rather than the reason for, severe amyloidosis.

In conclusion, these results indicate that apoA-I plays key roles in maintaining apoA-II distribution and HDL particle size. Furthermore, the redistribution of apoA-II may be the main reason for aggravated AApoAII amyloidosis in *Apoa1*$^{-/-}$ mice. ApoA-II may thus play important roles in substituting for the loss of apoA-I. These findings should provide novel insights for the relationship between apoA-I and apoA-II and the mechanism of amyloidosis.

REFERENCES

1. Kontush, A., and M. J. Chapman. 2006. Functionally defective HDL: a new therapeutic target at the crossroads of dyslipidemia, inflammation and atherosclerosis. *Pharmacol. Rev.* **58:** 342–374.
2. Chapman, M. J. 1980. Animal lipoproteins: chemistry, structure, and comparative aspects. *J. Lipid Res.* **21:** 789–853.
3. Sorci-Thomas, M. G., S. Bhat, and M. J. Thomas. 2009. Activation of lecithin:cholesterol acyltransferase by HDL ApoA-I central helices. *Clin. Lipidol.* **4:** 113–124.
4. Duffy, D., and D. J. Rader. 2009. Update on strategies to increase HDL quantity and function. *Nat. Rev. Cardiol.* **6:** 455–463.
5. Schaefer, E. J., R. D. Santos, and B. F. Asztalos. 2010. Marked HDL deficiency and premature coronary heart disease. *Curr. Opin. Lipidol.* **21:** 289–297.
6. Al-Sarraf, A., K. Al-Ghofaili, D. R. Sullivan, K. M. Wasan, R. Hegele, and J. Frohlich. 2010. Complete ApoAI deficiency in an Iraqi Mandaean family: case studies and review of the literature. *J. Clin. Lipidol.* **4:** 420–426.
7. Li, H., R. L. Reddick, and N. Maeda. 1993. Lack of apoA-I is not associated with increased susceptibility to atherosclerosis in mice. *Arterioscler. Thromb.* **13:** 1814–1821.
8. Kalopissis, A. D., and J. Chambaz. 2000. Transgenic animals with altered high-density lipoprotein composition and functions. *Curr. Opin. Lipidol.* **11:** 149–153.
9. Lee, M., L. Calabresi, G. Chiesa, G. Franceschini, and P. T. Kovanen. 2002. Mast cell chymase degrades apoE and apoA-II in apoA-I-knockout mouse plasma and reduces its ability to promote cellular cholesterol efflux. *Arterioscler. Thromb. Vasc. Biol.* **22:** 1475–1481.
10. Duverger, N., G. Tremp, J. M. Caillaud, F. Emmanuel, G. Castro, J. C. Fruchart, A. Steinmetz, and P. Denefle. 1996. Protection against atherogenesis in mice mediated by human apolipoprotein A-IV. *Science.* **273:** 966–968.
11. Blanco-Vaca, F., J. C. Escolà-Gil, J. M. Martín-Campos, and J. Julve. 2001. Role of apoA-II in lipid metabolism and atherosclerosis: advances in the study of an enigmatic protein. *J. Lipid Res.* **42:** 1727–1739.
12. Deeb, S. S., K. Takata, R. L. Peng, G. Kajiyama, and J. J. Albers. 1990. A splice-junction mutation responsible for familial apolipoprotein A-II deficiency. *Am. J. Hum. Genet.* **46:** 822–827.
13. Koike, T., S. Kitajima, Y. Yu, Y. Li, K. Nishijima, E. Liu, H. Sun, A. B. Waqar, N. Shibata, T. Inoue, et al. 2009. Expression of human apoAII in transgenic rabbits leads to dyslipidemia: a new model for combined hyperlipidemia. *Arterioscler. Thromb. Vasc. Biol.* **29:** 2047–2053.
14. Ge, F., J. Yao, X. Fu, Z. Guo, J. Yan, B. Zhang, H. Zhang, H. Tomozawa, J. Miyazaki, J. Sawashita, et al. 2007. Amyloidosis in transgenic mice expressing murine amyloidogenic apolipoprotein A-II (Apoa2c). *Lab. Invest.* **87:** 633–643.
15. Weng, W., and J. L. Breslow. 1996. Dramatically decreased high density lipoprotein cholesterol, increased remnant clearance, and insulin hypersensitivity in apolipoprotein A-II knockout mice suggest a complex role for apolipoprotein A-II in atherosclerosis susceptibility. *Proc. Natl. Acad. Sci. USA.* **93:** 14788–14794.
16. Castellani, L. W., A. M. Goto, and A. J. Lusis. 2001. Studies with apolipoprotein A-II transgenic mice indicate a role for HDLs in adiposity and insulin resistance. *Diabetes.* **50:** 643–651.
17. Thompson, P. A., J. F. Berbée, P. C. Rensen, and R. L. Kitchens. 2008. Apolipoprotein A-II augments monocyte responses to LPS by suppressing the inhibitory activity of LPS-binding protein. *Innate Immun.* **14:** 365–374.
18. Escolà-Gil, J. C., A. Marzal-Casacuberta, J. Julve-Gil, B. Y. Ishida, J. Ordóñez-Llanos, L. Chan, F. González-Sastre, and F. Blanco-Vaca. 1998. Human apolipoprotein A-II is a pro-atherogenic molecule when it is expressed in transgenic mice at a level similar to that in humans: evidence of a potentially relevant species-specific interaction with diet. *J. Lipid Res.* **39:** 457–462.
19. Warden, C. H., C. C. Hedrick, J. H. Qiao, L. W. Castellani, and A. J. Lusis. 1993. Atherosclerosis in transgenic mice overexpressing apolipoprotein A-II. *Science.* **261:** 469–472.
20. Benson, M. D., J. J. Liepnieks, M. Yazaki, T. Yamashita, A. K. Hamidi, B. Guenther, and B. Kluve-Beckerman. 2001. A new human hereditary amyloidosis: the result of a stop-codon mutation in the apolipoprotein AII gene. *Genomics.* **72:** 272–277.
21. Xing, Y., and K. Higuchi. 2002. Amyloid fibril proteins. *Mech. Ageing Dev.* **123:** 1625–1636.
22. Higuchi, K., J. Wang, K. Kitagawa, T. Matsushita, K. Kogishi, H. Naiki, H. Kitado, and M. Hosokawa. 1996. Accelerated senile amyloidosis induced by amyloidogenic Apoa-II gene shortens the life span of mice but does not accelerate the rate of senescence. *J. Gerontol. A Biol. Sci. Med. Sci.* **51:** B295–B302.
23. Kitagawa, K., J. Wang, T. Mastushita, K. Kogishi, M. Hosokawa, X. Fu, Z. Guo, M. Mori, and K. Higuchi. 2003. Polymorphisms of mouse apolipoprotein A-II: seven alleles found among 41 inbred strains of mice. *Amyloid.* **10:** 207–214.
24. Xing, Y., A. Nakamura, T. Korenaga, Z. Guo, J. Yao, X. Fu, T. Matsushita, K. Kogishi, M. Hosokawa, F. Kametani, et al. 2002. Induction of protein conformational change in mouse senile amyloidosis. *J. Biol. Chem.* **277:** 33164–33169.
25. Bekaert, E. D., P. Alaupovic, C. Knight-Gibson, R. A. Norum, M. J. Laux, and M. Ayrault-Jarrier. 1992. Isolation and partial characterization of lipoprotein A-II (LP-A-II) particles of human plasma. *Biochim. Biophys. Acta.* **1126:** 105–113.
26. Lefterov, I., N. F. Fitz, A. A. Cronican, A. Fogg, P. Lefterov, R. Kodali, R. Wetzel, and R. Koldamova. 2010. Apolipoprotein A-I deficiency increases cerebral amyloid angiopathy and cognitive deficits in APP/PS1DeltaE9 mice. *J. Biol. Chem.* **285:** 36945–36957.

27. Williamson, R., D. Lee, J. Hagaman, and N. Maeda. 1992. Marked reduction of high density lipoprotein cholesterol in mice genetically modified to lack apolipoprotein A-I. *Proc. Natl. Acad. Sci. USA.* **89:** 7134–7138.
28. Okazaki, M., S. Usui, M. Ishigami, N. Sakai, T. Nakamura, Y. Matsuzawa, and S. Yamashita. 2005. Identification of unique lipoprotein subclasses for visceral obesity by component analysis of cholesterol profile in high-performance liquid chromatography. *Arterioscler. Thromb. Vasc. Biol.* **25:** 578–584.
29. Umezawa, M., K. Tatematsu, T. Korenaga, X. Fu, T. Matushita, H. Okuyama, M. Hosokawa, T. Takeda, and K. Higuchi. 2003. Dietary fat modulation of apoA-II metabolism and prevention of senile amyloidosis in the senescence- accelerated mouse. *J. Lipid Res.* **44:** 762–769.
30. Higuchi, K., T. Yonezu, K. Kogishi, A. Matsumura, S. Takeshita, K. Higuchi, A. Kohno, M. Matsushita, M. Hosokawa, and T. Takeda. 1986. Purification and characterization of a senile amyloid-related antigenic substance (apoSASSAM) from mouse serum. apoSASSAM is an apoA-II apolipoprotein of mouse high density lipoproteins. *J. Biol. Chem.* **261:** 12834–12840.
31. Higuchi, K., A. Matsumura, A. Honma, S. Takeshita, K. Hashimoto, M. Hosokawa, K. Yasuhira, and T. Takeda. 1983. Systemic senile amyloid in senescence-accelerated mice. A unique fibril protein demonstrated in tissues from various organs by the unlabeled immunoperoxidase method. *Lab. Invest.* **48:** 231–240.
32. Korenaga, T., X. Fu, Y. Xing, T. Matsusita, K. Kuramoto, S. Syumiya, K. Hasegawa, H. Naiki, M. Ueno, T. Ishihara, et al. 2004. Tissue distribution, biochemical properties, and transmission of mouse type A AApoAII amyloid fibrils. *Am. J. Pathol.* **164:** 1597–1606.
33. Higuchi, K., H. Kitado, K. Kitagawa, K. Kogishi, H. Naiki, and T. Takeda. 1993. Development of congenic strains of mice carrying amyloidogenic apolipoprotein A-II (Apoa2c). Apoa2c reduces the plasma level and the size of high density lipoprotein. *FEBS Lett.* **317:** 207–210.
34. Zhang, H., J. Sawashita, X. Fu, T. Korenaga, J. Yan, M. Mori, and K. Higuchi. 2006. Transmissibility of mouse AApoAII amyloid fibrils: inactivation by physical and chemical methods. *FASEB J.* **20:** 1012–1014.
35. Fu, L., I. Matsuyama, T. Chiba, Y. Xing, T. Korenaga, Z. Guo, X. Fu, J. Nakayama, M. Mori, and K. Higuchi. 2001. Extrahepatic expression of apolipoprotein A-II in mouse tissues: possible contribution to mouse senile amyloidosis. *J. Histochem. Cytochem.* **49:** 739–748.
36. Castellani, L. W., M. Navab, B. J. Van Lenten, C. C. Hedrick, S. Y. Hama, A. M. Goto, A. M. Fogelman, and A. J. Lusis. 1997. Overexpression of apolipoprotein AII in transgenic mice converts high density lipoproteins to proinflammatory particles. *J. Clin. Invest.* **100:** 464–474.
37. Ribas, V., J. L. Sánchez-Quesada, R. Antón, M. Camacho, J. Julve, J. C. Escolà-Gil, L. Vila, J. Ordóñez-Llanos, and F. Blanco-Vaca. 2004. Human apolipoprotein A-II enrichment displaces paraoxonase from HDL and impairs its antioxidant properties: a new mechanism linking HDL protein composition and antiatherogenic potential. *Circ. Res.* **95:** 789–797.
38. Rotllan, N., V. Ribas, L. Calpe-Berdiel, J. M. Martín-Campos, F. Blanco-Vaca, and J. C. Escolà-Gil. 2005. Overexpression of human apolipoprotein A-II in transgenic mice does not impair macrophage-specific reverse cholesterol transport in vivo. *Arterioscler. Thromb. Vasc. Biol.* **25:** e128–e132.
39. Alaupovic, P., C. Knight-Gibson, C. S. Wang, D. Downs, E. Koren, H. B. Brewer, Jr., and R. E. Gregg. 1991. Isolation and characterization of an apoA-II-containing lipoprotein (LP-A-II:B complex) from plasma very low density lipoproteins of patients with Tangier disease and type V hyperlipoproteinemia. *J. Lipid Res.* **32:** 9–19.
40. Weers, P. M., A. B. Patel, L. C. Wan, E. Guigard, C. M. Kay, A. Hafiane, R. McPherson, Y. L. Marcel, and R. S. Kiss. 2011. Novel N-terminal mutation of human apolipoprotein A-I reduces self-association and impairs LCAT activation. *J. Lipid Res.* **52:** 35–44.
41. Zhou, H., Z. Li, D. L. Silver, and X. C. Jiang. 2006. Cholesteryl ester transfer protein (CETP) expression enhances HDL cholesteryl ester liver delivery, which is independent of scavenger receptor BI, LDL receptor related protein and possibly LDL receptor. *Biochim. Biophys. Acta.* **1761:** 1482–1488.
42. Hassan, W., H. Al-Sergani, W. Mourad, and R. Tabbaa. 2005. Amyloid heart disease. New frontiers and insights in pathophysiology, diagnosis, and management. *Tex. Heart Inst. J.* **32:** 178–184.
43. Higuchi, K., A. Matsumura, A. Honma, K. Toda, S. Takeshita, M. Matsushita, T. Yonezu, M. Hosokawa, and T. Takeda. 1984. Age-related changes of serum apoprotein SASSAM, apoprotein A-I and low-density lipoprotein levels in senescence accelerated mouse (SAM). *Mech. Ageing Dev.* **26:** 311–326.